Bmi1 promotes prostate tumorigenesis via inhibiting p16 and p14 expression

Catherine Fan, Lizhi He, Anil Kapoor, Aubrey Gillis, Adrian P. Rybak, Jean-Claude Cutz, Damu Tang

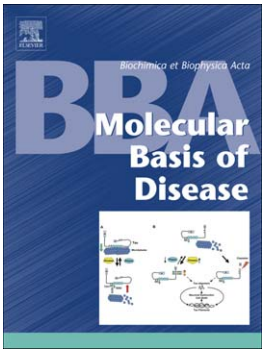

Bmi1 promotes prostate tumorigenesis via inhibiting $p16^{INK4A}$ and $p14^{ARF}$ expression

Catherine Fan, Lizhi He, Anil Kapoor, Aubrey Gillis, Adrian P. Rybak, Jean-Claude Cutz, Damu Tang

PII: S0925-4439(08)00161-0
DOI: doi: 10.1016/j.bbadis.2008.08.009
Reference: BBADIS 62844

To appear in: *BBA - Molecular Basis of Disease*

Received date: 18 May 2008
Revised date: 20 August 2008
Accepted date: 25 August 2008

Please cite this article as: Catherine Fan, Lizhi He, Anil Kapoor, Aubrey Gillis, Adrian P. Rybak, Jean-Claude Cutz, Damu Tang, Bmi1 promotes prostate tumorigenesis via inhibiting $p16^{INK4A}$ and $p14^{ARF}$ expression, *BBA - Molecular Basis of Disease* (2008), doi: 10.1016/j.bbadis.2008.08.009

Bmi1 promotes prostate tumorigenesis via inhibiting $p16^{INK4A}$ and $p14^{ARF}$ expression

Catherine Fan,[1,2] Lizhi He,[1,2] Anil Kapoor,[3#] Aubrey Gillis,[3] Adrian P. Rybak,[1,2] Jean-Claude Cutz,[4] Damu Tang [1,2#]

[1] Division of Nephrology, Department of Medicine, McMaster University and [2] Father Sean O'Sullivan Research Institute, St. Joseph's Hospital, Hamilton, ON, Canada [3] Department of Surgery and [4] Department of Pathology and Molecular Medicine, McMaster University, Hamilton, ON, Canada

#: Corresponding author:
Anil Kapoor
Tel: (905) 522-1155, ext. 33218
Fax: (905) 521-6195
Email: kapoor4@mcmaster.ca

Damu Tang
Tel: (905) 522-1155, ext. 35168
Fax: (905) 521-6181
Email: damut@mcmaster.ca

T3310, St. Joseph's Hospital
50 Charlton Ave East
Hamilton, ON
Canada L8N 4A6

Running title: Bmi1 promotes prostate tumorigenesis

Key words: Bmi1, $p16^{INK4A}$, $p14^{ARF}$, and Prostate Cancer

Abstract

We report here that the polycomb group protein Bmi1 promotes prostate tumorigenesis. Bmi1 is detected at higher levels in androgen-independent PC3 and DU145 than in androgen-dependent LNCaP prostate cancer (CaP) cells. Ectopic Bmi1 enhanced the expression of human telomerase reverse transcriptase (hTERT) and suppressed the exression of $p16^{INK4A}$ and $p14^{ARF}$ in CaP cells. Consistent with these observations, immunohistochemical staining of 51 cases of primary CaP specimens revealed 1.4 fold (p = 0.014) and 1.3 fold (p = 0.051) higher levels of Bmi1-positive cells in carcinoma compared to normal prostatic epithelial cells and PIN, respectively. In primary CaPs, Bmi1 expression was associated with a reduction in $p16^{INK4A}$ and $p14^{ARF}$. Furthermore, in comparison to empty vector-transfected cells, Bmi1-expressing DU145 cells formed significantly larger tumors in NOD/SCID mice. Taken together, we demonstrate that Bmi1 promotes prostate tumorigenesis.

1. Introduction

The polycomb group (PcG) *Bmi1* gene maintains the proliferative potential and self-renewal activity of hematopoietic and neural stem cells [1, 2]. This is in part attributable to Bmi1-mediated suppression of the transcription of $p16^{INK4A}$, $p19^{ARF}$/$p14^{ARF}$, and E4F1 [3, 4, 5]. This developmental function of Bmi1 is in line with its oncogenic role in leukemia. The *Bmi1* gene was initially isolated as an oncogene which cooperates with c-Myc in retrovirus-induced B and T cell leukemia [6, 7]. Overexpression of *Bmi1* transforms lymphocytes [8, 9] and was detected in 25% of mantle cell lymphoma [10]. Bmi1 positivity is associated with unfavorable prognosis in patients with diffuse large B cell lymphomas and myelodysplastic syndrome [11, 12]. Recently, increases in Bmi1 have also been reported in non-hematopoietic malignancies including non-small cell lung cancer (NSCLC) [13], colon cancer [14], medulloblastomas [15], breast cancer [16], and nasopharyngeal carcinoma [17].

Consistent with its role in inhibiting $p16^{INK4A}$ and $p19^{ARF}$ transcription, Bmi1 induces the bypassing of senescence. $Bmi1^{-/-}$ hematopoietic progenitors express increased $p16^{INK4A}$ and $p19^{ARF}$, and accumulate high levels of the senescence marker SA-β-Gal [5], consistent with the observed diminishing of self-renewal potential of $Bmi1^{-/-}$ hematopoietic stem cells [1]. $Bmi1^{-/-}$ mouse embryonic fibroblasts (MEFs) undergo premature senescence [18] and overexpression of *Bmi1* in MEFs and human fibroblasts extends their replicative life spans [18, 19]. Additionally, it has been shown that Bmi1 immortalizes human nasopharyngeal and mammary epithelial cells by enhancing human telomerase reverse transcriptase (hTERT) activity [17, 20].

A potential oncogenic role of Bmi1 has also been suggested in prostate cancer. Increases in *Bmi1* mRNA were detected in prostate cancer cell lines, xenografts derived from prostate cancer

cells and human primary prostate carcinoma, as well as mouse primary prostate tumors derived from the TRAMP transgenic mouse model [21]. Prostate cancer patients with an 11-gene signature, which is associated with Bmi1 expression, are likely to have unfavorable prognosis than those without this signature [21]. Additionally, metastatic prostate carcinoma precursor cells that are double-positive for Bmi1 and the polycomb-group protein EZH2 are more tumorigenic than those which are negative for both proteins [22]. However, the expression status of the Bmi1 protein in primary prostate cancer and the exact role of Bmi1 in prostate tumorigenesis have not been thoroughly investigated.

In this investigation, we have examined the Bmi1 protein in prostate cancer cell lines and in 51 cases of primary prostate cancer by immunohistochemistry. In comparison to normal prostatic epithelial cells, Bmi1 protein was expressed at higher levels in PINs and carcinomas. Additionally, a high level of Bmi1 is associated with reduction in $p16^{INK4A}$ and $p14^{ARF}$ in prostate carcinoma. This is in line with our in vitro study showing that ectopic Bmi1 reduces $p16^{INK4A}$ and $p14^{ARF}$ expression in DU145 prostate cancer cells and enhances DU145 cells to form xenograft tumors in immunocompromised mice. Taken together, our observations reveal that Bmi1 promotes prostate tumorigenesis, at least in part, by down-regulation of $p16^{INK4A}$ and $p16^{ARF}$.

2. Materials and Methods

2.1. Cell lines and plasmids

LNCaP, PC3, DU145, MCF7, HeLa, and 293T cells were purchased from ATCC, and cultured in RPMI-1640 (LNCaP), F12 (PC3), MEM (DU145), and DMEM (MCF7, HeLa, and 293T) plus 10% FBS and 1% Penicillin-Streptomycin (Invitrogen).

Human *Bmi1* cDNA was amplified by RT-PCR from HeLa cells, which was subsequently subcloned in pcDNA3 and pBabe retrovirus vectors. pGL3-hTERTmin-Luc reporter plasmid, containing a 59bp region of the hTERT promoter (-208 to -150) which has been shown to display maximal promoter activity [23], was constructed from HeLa cell genomic DNA using routine molecular biology techniques.

2.2. Retroviral Infection

Retroviral infection was performed following our published procedure [24, 25]. Briefly, a gag-pol expressing vector and an envelope-expressing vector (VSV-G) (Stratagene) were transiently co-transfected with a designed retroviral plasmid into 293T cells. After 48 hours, the virus-containing medium was harvested, filtered through a 0.45μM filter, and centrifuged at 50,000g for 90 minutes to concentrate the retrovirus. Following the addition of 10 μg/ml of polybrene (Sigma), the medium was used to infect cells. Infection for pBabe-based constructs was selected in puromycin, while infection for pLHCX-based constructs was selected in hygromycin.

2.3. Collecting primary prostate cancer

Prostate tissue was collected from patients who underwent radical prostactomy at St. Joseph's Hospital in Hamilton, Ontario, Canada under the approval from the local Ethics Board and consent from patients. The patient cohort (51 CaP patients) used in this investigation represents the typical patient population treated in this center. Cancers were examined and graded by pathologists of the Hospital. 51 primary prostate cancer specimens were collected. All patients in our cohort have not received hormonal and radiation therapies prior to surgery. Information regarding these specimens is presented in Table 1.

2.4. Western blot

Cell lysates were prepared and western blot was performed according to our published procedure [24]. 50μg protein of total lysate was separated on SDS-PAGE gel and transferred onto Immobilon-P membranes (Millipore). Membranes were blocked with 5% skim milk and then incubated with the indicated antibodies at room temperature for 1 hour. Signals were detected using an ECL Western Blotting Kit (Amersham). Primary antibodies used were: polyclonal anti-Bmi1 (1:100, Santa Cruz Biotechnology), polyclonal anti-$p16^{INK4A}$ (1:500, Santa Cruz Biotechnology), and polyclonal anti-$p14^{ARF}$ (1:5000, Sigma).

2.5. Immunofluorescence and Immunohistochemistry of Bmi1, $p16^{INK4A}$, and $p14^{ARF}$ as well as statistical analysis

Immunofluorescence staining was carried out using the following antibodies: a monoclonal anti-FLAG (M2, 1:500; Sigma), anti-Bmi1, and FITC-Donkey anti-mouse IgG

(1:200; Jackson Immuno Research). Images were captured using Axiovert 200M and AxioVision 3 software.

Immunohistochemistry (IHC) was performed on 51 paraffin-embedded, serially-cut prostate cancer tissues. IHC procedure was optimized and did not produce detectable artificial staining that might be associated with antigen-retrieval and fixation, as control IgG (negative control) did not generate detectable staining (Fig 2). Briefly, slides were deparaffinized in xylene, cleared in ethanol series, and heat-treated for 30 minutes in sodium citrate buffer (pH = 6.0) in a food steamer. Primary antibodies specific for Bmi1 (1:100, Santa Cruz Biotechnology), $p16^{INK4A}$ (1:100, Santa Cruz Biotechnology), and $p14^{ARF}$ (1:1000, Sigma) were incubated with the sections overnight at 4°C. Negative controls were incubated with a non-specific anti-rabbit IgG. Biotinylated goat anti-rabbit IgG and Vector ABC reagent (Vector Laboratories) were subsequently added according to the manufacturer's instructions. Washes were performed with Tris-buffered saline containing 0.1% Tween-20 (TBST). Chromogen reaction was carried out with diaminobenzidine, and counterstaining was done with hematoxylin. Hematoxylin and eosin (H&E) staining was carried out using a standard protocol.

Analysis of immunohistochemistry was performed using Northern Eclipse 4.0 software (manual cell counter) for Windows. Approximately 1000 cells from randomly selected fields were counted for each normal, PIN, and cancer foci per patient. Mean percentages of positively-stained cells were then analyzed using GraphPad 4.0 for Windows.

2.6. Generation of xenograft tumors in NOD/SCID mice

DU145 cells were enzymatically dissociated, resuspended in serum-containing MEM/Matrigel mixture (1:1 volume), and kept at 4°C until injection. An amount equal to 0.1 ml, containing 2 x 10^5 cells, was subcutaneously injected into each flank of 8-week-old male NOD SCID mice (The Jackson Laboratory, Bar Harbor, Maine) using a 25-gauge needle, for a total of 4 mice for each cell line. Mice were inspected for tumor appearance, by observation and palpation, and tumor growth was measured weekly using a caliper. Tumor volume was determined using the standard formula: $L \times W^2 \times 0.52$, where L and W are the longest and shortest diameters, respectively. The presence of each tumor nodule was confirmed by necropsy. All animal work was carried out according to experimental protocols approved by the McMaster University Animal Research Ethics Board.

3. Results

3.1. Increases in Bmi1 protein in prostate cancer

To investigate an oncogenic role of Bmi1 in prostate cancer, we first examined the Bmi1 protein in the three most widely used CaP cell lines, androgen-dependent LNCaP and androgen-independent PC3 and DU145 cells. While the presence of Bmi1 in PC3 and DU145 cells was readily detected, we could not detect the Bmi1 protein in LNCaP cells (Fig. 1A) even after prolonged exposure and using double the amount of total cell lysate (100 μg) (50 μg cell lysates were used for other lines, Fig. 1A). Although approximately two-fold less *Bmi1* mRNA was reported in LNCaP than in PC3 cells [21], our results suggest that LNCaP cells express a substantially low (or undetectable) level of Bmi1 protein. Immunofluorescence (IF) detected

Bmi1 protein in the nucleus of PC3, DU145, and MCF7 cells, but not in the nucleus of LNCaP cells (Fig. 1B).

We have further examined Bmi1 expression in primary CaPs. Immunohistochemistry (IHC) staining of 51 primary CaP specimens detected Bmi1 in normal prostate glands, PIN (data not shown), and carcinoma (Fig. 2). To quantify the percentage of cells expressing Bmi1, we have counted 1000 cells in individual tissues (normal prostate glands, PINs, and carcinomas) for each of the 51 primary CaP specimens. For each specimen, an average of 27.8% of epithelial cells in normal prostatic glands and 30.9% in PIN tissues expressed Bmi1, while a significant 11.3% increase in Bmi1-positive cells was observed in carcinoma (Table 2). This pattern of Bmi1 expression is in line with the pattern of CBX7 expression, a PcG member, in prostate cancer [26]. Taken together, we demonstrate increased levels of Bmi1 protein in CaP, which is consistent with the reported increases in *Bmi1* mRNA in prostate cancer [21].

3.2. Bmi1 suppresses $p16^{INK4A}$ and $p14^{ARF}$ expression as well as enhances hTERT expression in prostate cancer

Bmi1 has been shown to inhibit the transcription of $p16^{INK4A}$ and $p14^{ARF}$ [3, 4]. To examine whether this is also the case in prostate cancer, we have stably-expressed Bmi1 in DU145, PC3, and LNCaP cells. Ectopic Bmi1 led to a modest decrease in endogenous $p16^{INK4A}$, which may be attributable to the DU145 cell expressing mutant $p16^{INK4A}$ [27], and a clear reduction in endogenous $p14^{ARF}$ in DU145 and PC3, but not LNCaP (Fig. 3A, top panels). Ectopic Bmi1 was expressed slightly higher than endogenous Bmi1 in DU145 and PC3 cells, evidenced by a slight one-fold increase in Bmi1 protein detected in Bmi1-transfected cells than in empty vector

(pBabe) transfected cells (Fig. 3A, bottom panels). Thus, the reduction of $p16^{INK4A}$ and $p14^{ARF}$ in PC3 and DU145 cells by ectopic Bmi1 was not due to very high levels of ectopic Bmi1. The fact that we did not observe decreases in $p16^{INK4A}$ and $p14^{ARF}$ in LNCaP cells may be attributable to these cells expressing very low levels of endogenous Bmi1, $p16^{INK4A}$ and $p14^{ARF}$ proteins (Fig. 3A).

Bmi1 has been reported to induce hTERT expression in mammary epithelial cells [20]. To address whether Bmi1 modulates hTERT expression, we co-transfected a hTERT promoter reporter construct (pGL3-hTERTmin-Luc) [23] together with Bmi1. In comparison to the empty vector control, Bmi1 up-regulates hTERT expression (Fig. 3B).

3.3. Bmi1 positivity is associated with reduction in $p16^{INK4A}$ and $p14^{ARF}$ in primary prostate cancer

To determine whether Bmi1 is associated with the reduction of $p16^{INK4A}$ and $p14^{ARF}$ in primary CaP, we have examined the expression of Bmi1, $p16^{INK4A}$, and $p14^{ARF}$ proteins in 51 primary prostate cancer tissues. All three proteins largely express in both basal and luminal epithelial cells of prostate glands, with occasional staining detected in the stroma (Fig 2). Furthermore, we were able to locate the expression of Bmi1, $p16^{INK4A}$ and $p14^{ARF}$ to the same regions by staining serially-cut slides (Fig 2). In each specimen, normal prostatic glands, high-grade PINs, and carcinomas were located. In tissues derived from the same patient, high levels of Bmi1 were associated with decreases in $p16^{INK4A}$ in normal prostatic glands (Fig. 2), whereas low levels of Bmi1 were associated with high levels of $p16^{INK4a}$ in PINs (Fig. 2). The Bmi1-positive carcinomas also expressed reduced $p16^{INK4A}$ (Fig. 2). In terms of $p14^{ARF}$, while Bmi1

positivity did not associate with $p14^{ARF}$ reduction in normal prostate glands, the presence of Bmi1 associated with decreases in $p14^{ARF}$ in PINs and carcinoma (Fig. 2, Table 3). By comparing the mean percentages of cells stained in normal prostatic glands, PINs, and carcinomas for each individual specimen using *t*-tests, it was revealed that Bmi1-positive cells associated with significant $p16^{INK4A}$ reduction in normal ($p < 0.05$) and PIN ($p < 0.05$) tissues (Table 3). This inverse correlation was also confirmed by Pearson correlation tests (data not shown). Among the epithelial cells present in normal and PIN tissues, 25% and 75% of Bmi1-positive cells are $p16^{INK4A}$ positive and negative, respectively, compared to 52.4% and 47.6% of Bmi1-negative normal epithelial cells being $p16^{INK4A}$ positive and negative, respectively, and 65.5% and 34.5% of Bmi1-negative PIN cells being $p16^{INK4A}$ positive and negative, respectively (Table 3). This inverse expression pattern between Bmi1 and $p16^{INK4A}$ suggests that Bmi1 inhibits $p16^{INK4A}$ in normal prostatic glands and PINs. However, this inverse relationship was not observed in prostate carcinoma (Table 3). An overall 74% of carcinoma cells expressed no detectable $p16^{INK4A}$ in both Bmi1-positive and negative carcinoma (Table 3). However, it is clear that loss of this inverse relationship in carcinoma is not because of changes in the ratio between $p16^{INK4A}$ positive and $p16^{INK4A}$ negative populations in Bmi1-positive carcinoma, as this ratio remains comparable in normal prostatic glands, PINs, and carcinomas (Table 3), but rather due to increases in $p16^{INK4A}$ negative cells in Bmi1-negative carcinoma (Table 3). This would strongly suggest that additional mechanisms have developed in carcinoma to reduce $p16^{INK4A}$ expression. Consistent with this inference, *t*-test analysis of $p16^{INK4A}$ positive and $p16^{INK4A}$ negative populations in Bmi1-positive carcinoma revealed that the difference between these two populations is statistically significant ($p < 0.009$, data not shown).

Analysis of Bmi1 and $p14^{ARF}$ expression in primary CaP tissues demonstrated that Bmi1 did not inhibit $p14^{ARF}$ expression in normal prostate epithelial cells (Table 3). However, Bmi1 suppresses $p14^{ARF}$ expression in both PIN and carcinoma tissues, as an inverse relationship between Bmi1-positive and $p14^{ARF}$ negative expression was observed (Table 3). Taken together, we provide evidence indicating that Bmi1 plays a role in inhibiting $p16^{INK4A}$ expression in normal prostate epithelial cells and PINs, and in inhibiting $p14^{ARF}$ expression in PIN and carcinoma tissues (Table 3). The fact that Bmi1 only reduces $p14^{ARF}$ in precancerous lesions (PINs) and carcinomas is consistent with the established role of $p14^{ARF}$ in tumor surveillance during tumorigenesis, as $p14^{ARF}$ will not be fully functional in normal cells [28]. Collectively, these observations support the notion that Bmi1 promotes CaP tumorigenesis by inhibiting $p16^{INK4A}$ and $p14^{ARF}$ expression.

3.4. Bmi1 sensitizes DU145 cells to form xenograft tumors in immunocompromised mice

Although DU145 cells express mutant $p16^{INK4A}$ [27], the aforementioned observations that Bmi1 suppresses $p14^{ARF}$ and enhances hTERT expression in DU145 cells suggest that Bmi1 may promote DU145 cells to form tumors in immunocompromised mice. To examine this possibility, we have subcutaneously (s.c.) implanted $2x10^5$ empty vector (EV) or Bmi1 stably expressing DU145 cells into NOD/SCID mice (4 mice for each of EV and Bmi1-overexpressing cell lines). In comparison to EV cells, Bmi1 DU145 cells formed larger tumors (Table 4). When cultured as a monolayer, DU145 cell proliferation was not enhanced by ectopic Bmi1 expression (data not shown). Taken together, the above observations support the concept that Bmi1 promotes prostate

tumorigenesis via down-regulation of tumor suppressors ($p16^{INK4A}$ and $p14^{ARF}$) and up-regulation of hTERT.

4. Discussion

Bmi1 has recently been shown to immortalize mammary and nasopharyngeal epithelial cells by upregulating hTERT and inhibiting $p16^{INK4A}$, thereby promoting the formation of epithelial malignancies [20, 17]. This is consistent with the observed increases in *Bmi1* mRNA in primary prostate cancer (an epithelial malignancy) [21]. However, whether Bmi1 functions in prostate tumorigenesis has not yet been fully investigated.

We show that elevated levels of Bmi1 protein are present in prostate cancer. High levels of Bmi1 protein were detected in androgen-independent PC3 and DU145 CaP cells compared to androgen-dependent LNCaP cells (Fig. 1). In primary prostate carcinoma, immunohistochemistry (Table 2) revealed increases in Bmi1 in carcinoma cells when compared to normal prostatic epithelial cells. A similar situation has also been reported for another PcG protein, CBX7 [26].

Bmi1 promotes CaP tumorigenesis by inhibiting the *INK4A/ARF* locus. This locus on human chromosome 9p21 encodes $p16^{INK4A}$ and $p14^{ARF}$ by alternative splicing and the use of different reading frames [29]. Methylation of the $p14^{ARF}$ promoter has been detected in primary CaP [30]. While loss of $p16^{INK4A}$ function has been observed in a variety of cancers via homozygous deletion and promoter methylation [31, 32], the status of $p16^{INK4A}$ expression in CaP is complex. Mutation of the $p16^{INK4A}$ gene in CaP is not a frequent event [33]. Methylation of $p16^{INK4A}$ was associated with the reduction of $p16^{INK4A}$ mRNA and protein in primary prostate cancer [27, 34].

This event has been reported to occur in 43% [27], 66% [35], and 80.9% [30] of primary CaP. Paradoxically, overexpression of $p16^{INK4A}$ has also been observed in 43% [36], 65% [37], and 83% [38] of primary CaP. In all of these studies, overexpression of $p16^{INK4A}$ was associated with adverse prognosis. These discrepancies are most likely caused by the heterogeneous nature of prostate cancer. By counting 1000 cells within normal prostate glands, PINs, and carcinomas for all 51 primary CaP specimens, we conclusively demonstrate that 74% of carcinomas expressed undetectable $p16^{INK4A}$ protein (Table 3). While Bmi1 may play a major role in inhibiting $p16^{INK4A}$ in normal prostate glands and PINs, Bmi1, along with additional mechanisms, may also be in place to suppress $p16^{INK4A}$ in carcinomas (Table 3), suggesting that maintaining $p16^{INK4A}$ suppression is important for CaP formation. In our primary CaP specimens, $p16^{INK4A}$ staining was detected exclusively in the nucleus, suggesting $p16^{INK4A}$ as being functional. Our prostate carcinomas were within a narrow range of Gleason scores, with the majority having scores of 6-7 (Table 1). 26% of our carcinomas expressed $p16^{INK4A}$, an observation consistent with a recent report showing 25% of low-grade carcinomas being $p16^{INK4A}$ positive [39]. Additionally, Bmi1 also inhibits $p14^{ARF}$ in PINs and carcinoma (Table 3). However, Bmi1 does not play a role in inhibiting $p14^{ARF}$ expression in normal prostatic epithelial cells (Table 3). This may be attributable to the fact that ARF plays a major role in oncogene-provoked tumor surveillance [28]. The lack of oncogenic signals, including the Bmi1 signal, in normal prostatic epithelial cells may underlie the reason why Bmi1 does not contribute to reducing $p14^{ARF}$ expression in these cells. Taken together, our observations suggest that Bmi1 reduces *INK4A/ARF* expression during the evolution of CaP formation from normal epithelial cells to PIN and carcinoma.

Acknowledgements

We thank Drs. Xinchang Feng and Lieqi Liu for their excellent technical support. C.F. is supported by studentship from FSORC, St. Joseph's Hospital, Hamilton, Ontario, Canada. This work was supported by grants from the Prostate Cancer Research Foundation of Canada to DT (2005-2007, 2007-2008).

References

[1] I.K. Park, D. Qian, M. Kiel, M.W. Becker, M. Pihalja, I.L. Weissman, S.J. Morrison, M.F. Clarke, Bmi-1 is required for maintenance of adult self-renewing haematopoietic stem cells. Nature 423 (2003) 302-305.

[2] A.V. Molofsky, R. Pardal, T. Iwashita, I.K. Park, M.F. Clarke, S.J. Morrison, Bmi-1 dependence distinguishes neural stem cell self-renewal from progenitor proliferation. Nature 425 (2003) 962-967.

[3] S.W. Bruggeman, M.E. Valk-Lingbeek, P.P. van der Stoop, J.J. Jacobs, K. Kieboom, E. Tanger, D. Hulsman, C. Leung, Y. Arsenijevic, S. Marino, M. van Lohuizen, Ink4a and Arf differentially affect cell proliferation and neural stem cell self-renewal in Bmi1-deficient mice. Genes Dev 19 (2005) 1438-1443.

[4] A.V. Molofsky, S. He, M. Bydon, S.J. Morrison, R. Pardal, Bmi-1 promotes neural stem cell self-renewal and neural development but not mouse growth and survival by repressing the p16Ink4a and p19Arf senescence pathways. Genes Dev 19 (2005) 1432-1437.

[5] J. Chagraoui, S.L. Niessen, J. Lessard, S. Girard, P. Coulombe, M. Sauvageau, S. Meloche, G. Sauvageau, E4F1: a novel candidate factor for mediating BMI1 function in primitive hematopoietic cells. Genes Dev 20 (2006) 2110-2120.

[6] Y. Haupt, W.S. Alexander, G. Barri, S.P. Klinken, J.M. Adams, Novel zinc finger gene implicated as myc collaborator by retrovirally accelerated lymphomagenesis in E mu-myc transgenic mice. Cell 65 (1991) 753-763.

[7] M. van Lohuizen, S. Verbeek, B. Scheijen, E. Wientjens, H. van der Gulden, A. Berns, Identification of cooperating oncogenes in E mu-myc transgenic mice by provirus tagging. Cell 65 (1991) 737-752.

[8] Y. Haupt, M.L. Bath, A.W. Harris, J.M. Adams, bmi-1 transgene induces lymphomas and collaborates with myc in tumorigenesis. Oncogene 8 (1993) 3161-3164.

[9] M.J. Alkema, H. Jacobs, M. van Lohuizen, A. Berns, Pertubation of B and T cell development and predisposition to lymphomagenesis in Emu Bmi1 transgenic mice require the Bmi1 RING finger. Oncogene 15 (1997) 899-910.

[10] S. Bea, F. Tort, M. Pinyol, X. Puig, L. Hernández, S. Hernández, P.L. Fernandez, M. van Lohuizen, D. Colomer, E. Campo, BMI-1 gene amplification and overexpression in hematological malignancies occur mainly in mantle cell lymphomas. Cancer Res 61 (2001) 2409-2412.

[11] J.C. van Galen, J.J. Muris, J.J. Oudejans, W. Vos, C.P. Giroth, G.J. Ossenkoppele, A.P. Otte, F.M. Raaphorst, C.J. Meijer, Expression of the polycomb-group gene BMI1 is related to an unfavourable prognosis in primary nodal DLBCL. J Clin Pathol 60 (2007) 167-172.

[12] K. Mihara, M. Chowdhury, N. Nakaju, S. Hidani, A. Ihara, H. Hyodo, S. Yasunaga, Y. Takihara, A. Kimura, Bmi-1 is useful as a novel molecular marker for predicting progression of myelodysplastic syndrome and patient prognosis. Blood 107 (2006) 305-308.

[13] S. Vonlanthen, J. Heighway, H.J. Altermatt, M. Gugger, A. Kappeler, M.M. Borner, M. van Lohuizen, D.C. Betticher, The bmi-1 oncoprotein is differentially expressed in non-small cell lung cancer and correlates with INK4A-ARF locus expression. Br J Cancer 84 (2001)1372-1376.

[14] J.H. Kim, S.Y. Yoon, C.N. Kim, J.H. Joo, S.K. Moon, I.S. Choe, Y.K. Choe, J.W. Kim, The Bmi-1 oncoprotein is overexpressed in human colorectal cancer and correlates with the reduced p16INK4a/p14ARF proteins. Cancer Lett 203 (2004) 217-224.

[15] C. Leung, M. Lingbeek, O. Shakhova, J. Liu, E. Tanger, P. Saremaslani, M. Van Lohuizen, S. Marino, Bmi1 is essential for cerebellar development and is overexpressed in human medulloblastomas. Nature 428 (2004) 337-341.

[16] J.H. Kim, S.Y. Yoon, S.H. Jeong, S.Y. Kim, S.K. Moon, J.H. Joo, Y. Lee, I.S. Choe, J.W. Kim, Overexpression of Bmi-1 oncoprotein correlates with axillary lymph node metastases in invasive ductal breast cancer. Breast 13 (2004) 383-388.

[17] L.B. Song, M.S. Zeng, W.T. Liao, L. Zhang, H.Y. Mo, W.L. Liu, J.Y. Shao, Q.L. Wu, M.Z. Li, Y.F. Xia, L.W. Fu, W.L. Huang, G.P. Dimri, V. Band, Y.X. Zeng, Bmi-1 is a novel molecular marker of nasopharyngeal carcinoma progression and immortalizes primary human nasopharyngeal epithelial cells. Cancer Res 66 (2006) 6225-6232.

[18] J.J. Jacobs, K. Kieboom, S. Marino, R.A. DePinho, M. van Lohuizen, The oncogene and Polycomb-group gene bmi-1 regulates cell proliferation and senescence through the ink4a locus. Nature 397 (1999) 164-168.

[19] K. Itahana, Y. Zou, Y. Itahana, J.L. Martinez, C. Beausejour, J.J. Jacobs, M. Van Lohuizen, V. Band, J. Campisi, G.P. Dimri, Control of the replicative life span of human fibroblasts by p16 and the polycomb protein Bmi-1. Mol Cell Biol 23 (2003) 389-401.

[20] G.P. Dimri, J.L. Martinez, J.J. Jacobs, P. Keblusek, K. Itahana, M. Van Lohuizen, J. Campisi, D.E. Wazer, V. Band, The Bmi-1 oncogene induces telomerase activity and immortalizes human mammary epithelial cells. Cancer Res 62 (2002) 4736-4745.

[21] G.V. Glinsky, O. Berezovska, A.B. Glinskii, Microarray analysis identifies a death-from-cancer signature predicting therapy failure in patients with multiple types of cancer. J. Clin Invest 115 (2005) 1503-1521.

[22] O.P. Berezovska, A.B. Glinskii, Z. Yang, X.M. Li, R.M. Hoffman, G.V. Glinsky, Essential role for activation of the Polycomb group (PcG) protein chromatin silencing pathway in metastatic prostate cancer. Cell Cycle 5 (2006) 1886-1901.

[23] I. Horikawa, P.L. Cable, C. Afshari, J.C. Barrett, Cloning and characterization of the promoter region of human telomerase reverse transcriptase gene. Cancer Res 59 (1999) 826-830.

[24] D. Tang, H. Okada, J. Ruland, L. Liu, V. Stambolic, T.W. Mak, A.J. Ingram, Akt is activated in response to an apoptotic signal. J Biol Chem 276 (2001) 30461-30466.

[25] Y. Li, D. Wu, B. Chen, A. Ingram, L. He, L. Liu, D. Zhu, A. Kapoor, D. Tang, ATM activity contributes to the tumor suppressing functions of $p14^{ARF}$. Oncogene 23 (2004) 7355-7365.

[26] D. Bernard, J.F. Martinez-Leal, S. Rizzo, D. Martinez, D. Hudson, T. Visakorpi, G. Peters, A. Carnero, D. Beach, J. Gil, CBX7 controls the growth of normal and tumor-derived prostate cells by repressing the Ink4a/Arf locus. Oncogene 24 (2005) 5543-5551.

[27] S.G. Chi, R.W. deVere White, J.T. Muenzer, P.H. Gumerlock, Frequent alteration of CDKN2 (p16(INK4A)/MTS1) expression in human primary prostate carcinomas. Clin Cancer Res 3 (1997) 1889-1897.

[28] C.J. Sherr, Tumor surveillance via the ARF-p53 pathway. Genes Dev. 12 (1998) 2984-2991.

[29] D.E. Quelle, F. Zindy, R.A. Ashmun, C.J. Sherr, Alternative reading frames of the INK4a tumor suppressor gene encode two unrelated proteins capable of inducing cell cycle arrest. Cell 83 (1995) 993-1000.

[30] M.O. Hoque, O. Topaloglu, S. Begum, R. Henrique, E. Rosenbaum, W. Van Criekinge, W.H. Westra, D. Sidransky, Quantitative methylation-specific polymerase chain reaction gene patterns in urine sediment distinguish prostate cancer patients from control subjects. J Clin Oncol 23 (2005) 6569-6579.

[31] P. Cairns, T.J. Polascik, Y. Eby, K. Tokino, J. Califano, A. Merlo, L. Mao, J. Herath, R. Jenkins, W. Westra, et al., Frequency of homozygous deletion at p16/CDKN2 in primary human tumours. Nat Genet 11 (1995) 210-212.

[32] J.G. Herman, A. Merlo, L. Mao, R.G. Lapidus, J.P. Issa, N.E. Davidson, D. Sidransky, S.B. Baylin, Inactivation of the CDKN2/p16/MTS1 gene is frequently associated with

aberrant DNA methylation in all common human cancers. Cancer Res 55 (1995) 4525-4530.

[33] D.I. Quinn, S.M. Henshall, R.L. Sutherland, Molecular markers of prostate cancer outcome. Eur J Cancer 41 (2005) 858-887.

[34] N. Konishi, M. Nakamura, M. Kishi, M. Nishimine, E. Ishida, K. Shimada, Heterogeneous methylation and deletion patterns of the INK4a/ARF locus within prostate carcinomas. Am J Pathol 160 (2002) 1207-1214.

[35] N. Konishi, M. Nakamura, M. Kishi, M. Nishimine, E. Ishida, K. Shimada, DNA hypermethylation status of multiple genes in prostate adenocarcinomas. Jpn J Cancer Res 93 (2002) 767-773.

[36] C.T. Lee, P. Capodieci, I. Osman, M. Fazzari, J. Ferrara, H.I. Scher, C. Cordon-Cardo, Overexpression of the cyclin-dependent kinase inhibitor p16 is associated with tumor recurrence in human prostate cancer. Clin Cancer Res 5 (1999) 977-983.

[37] S.M. Henshall, D.I. Quinn, C.S. Lee, D.R. Head, D. Golovsky, P.C. Brenner, W. Delprado, P.D. Stricker, J.J. Grygiel, R.L. Sutherland, Overexpression of the cell cycle inhibitor p16INK4A in high-grade prostatic intraepithelial neoplasia predicts early relapse in prostate cancer patients. Clin Cancer Res 7 (2001) 544-550.

[38] D.F. Jarrard, J. Modder, P. Fadden, V. Fu, L. Sebree, D. Heisey, S.R. Schwarze, A. Friedl, Alterations in the p16/pRb cell cycle checkpoint occur commonly in primary and metastatic human prostate cancer. Cancer Lett 185 (2002) 191-199.

[39] Z. Zhang, D.G. Rosen, J.L. Yao, J. Huang, J. Liu, Expression of p14ARF, p15INK4b, p16INK4a, and DCR2 increases during prostate cancer progression. Mod Pathol 19 (2006) 1339-1343.

Figure legends

Fig. 1. Expression of Bmi1 in prostate cancer cells. (A) LNCaP, PC3, DU145, and MCF7 (breast cancer cells) cells were examined for Bmi1 expression by western blot. (B) IF staining of LNCaP, PC3, DU145, and MCF7 cells for Bmi1 protein. Nuclei were counter-stained with DAPI (blue). Scale bar represents 10 μM.

Fig. 2. Expression of Bmi1 protein in primary prostate cancer tissues associates with reduction in $p16^{INK4A}$ and $p14^{ARF}$. H&E (HE) and immunohistochemical (IHC) staining of normal prostatic gland (Normal), PIN, and carcinoma with Bmi1-, $p16^{INK4A}$- and $p14^{ARF}$ specific antibodies or control IgG (IgG). All tissues were from the same patient/slide. Scale bar represents 40 μM. The inset areas are enlarged.

Fig. 3. Bmi1 inhibits the expression of $p16^{INK4A}$ and $p14^{ARF}$ and enhances hTERT expression in prostate cancer cells. (A) DU145, PC3, and LNCaP cells were stably transfected with empty retrovirus (pBabe) or Bmi1 retrovirus. Bmi1 expression was examined by western blot using anti-FLAG and anti-Bmi1 (αBmi1) antibodies. The expression of $p16^{INK4A}$, $p14^{ARF}$, and actin was also examined by western blot using specific antibodies. (B) 293T cells were transiently transfected with empty vector or Bmi1 (as indicated) with a hTERT promoter-driven luciferase construct plus a β-Gal construct for 48 hours. Luciferase and β-Gal enzymatic activities were determined. Luciferase activities were normalized against β-Gal activities. Each transfection was carried out in triplicate and the experiment was repeated twice.

Table 1. Prostate cancer specimens used in this investigation

Patient	Age	Gleason	Capsule Involvement	pT	Perineural Invasion	pN	PSA (ng/mL)
1	62	3+3	No	pT2c	Unknown	pNX	7.66
2	68	3+3	Yes	pT2c	Yes	pN0	Unknown
3	61	3+4	No	pT2c	Unknown	pN0	5.67
4	57	3+4	Yes	pT2c	Unknown	pN0	4.6
5	58	3+3	No	pT2c	Unknown	pN0	7.2
6	67	3+5	No	pT2c	Yes	pN0	5.8
7	57	3+3	Yes	pT3b	Yes	pNX	7.49
8	70	4+4	No	pT2c	Unknown	pN0	21
9	61	3+4	Yes	pT3a	Unknown	pNX	4.98
10	56	3+3	No	pT2c	Unknown	pNX	Unknown
11	60	4+3	Yes	pT3a	Unknown	pN0	7.8
12	50	4+3	No	pT2c	Unknown	pN0	13
13	69	3+4	Yes	pT3b	Yes	pNX	3.7
14	67	3+4	No	pT2c	Unknown	pNX	5.01
15	58	3+3	No	pT2c	Unknown	pNX	13.58
16	61	4+3	Yes	pT3a	Yes	pN0	24.07
17	52	3+3	Yes	pT3b	Unknown	pN0	Unknown
18	68	3+4	Yes	pT3a	Yes	pN0	4.4
19	65	3+3	No	pT2c	No	pNX	4.4
20	66	3+4	No	pT2c	Unknown	pN0	6.7
21	74	3+4	No	pT2c	Yes	pNX	Unknown
22	62	3+4	No	pT2c	Unknown	pN0	5.16
23	62	3+4	No	pT2c	Yes	pN0	4.48
24	63	3+4	Yes	pT3a	Yes	pN0	8.7
25	67	3+3	No	pT2a	Unknown	pNX	8.3
26	67	3+5	No	pT2c	Yes	pN0	5.2
27	60	3+4	Yes	pT2c	Unknown	pNX	5.1
28	59	3+3	Yes	pT2c	Yes	pNX	5.69
29	65	3+3	No	pT2c	Yes	pNX	5.48
30	50	3+4	No	pT2c	Yes	pN0	6.4
31	64	3+4	Yes	pT3a	Yes	pN0	9.69
32	51	3+4	No	pT2a	Unknown	pNX	5.6
33	57	3+4	No	pT2c	Unknown	pN0	20
34	67	3+3	No	pT2c	Yes	pN0	5.01
35	53	3+4	Yes	pT3a	Unknown	pNX	8.68
36	56	3+4	No	pT2c	Unknown	pNX	Unknown
37	65	3+4	Yes	pT2c	Yes	pNX	5.07
38	69	3+5	Yes	pT3a	Yes	pN0	6.7
39	60	3+4	No	pT2c	Yes	pN0	9.86
40	58	3+4	No	pT2c	Unknown	pNX	4.2
41	68	4+3	Yes	pT3a	Yes	pN0	20
42	61	3+4	No	pT2c	No	pNX	7.6
43	54	4+3	Yes	pT3b	Yes	pN0	12
44	56	3+4	Yes	pT2c	Unknown	pN0	9.7
45	65	4+4	No	pT2a	Yes	pNX	8
46	55	3+3	Yes	pT2a	Unknown	pNX	6.17
47	58	3+3	No	pT2c	Unknown	pNX	5.32
48	73	4+3	No	pT2c	Unknown	pNX	5.2
49	64	3+3	No	pT2a	Unknown	pN0	7.9
50	67	3+3	No	pT2c	Unknown	pNX	5.89
51	60	3+3	No	pT2c	Unknown	pN0	6.7

Table 2. Bmi1 positive cells in primary prostate cancer

Normal	27.8 ± 3.1%
PIN	30.9 ± 5.2%
Carcinoma	39.1 ± 3.2%

Note: Mann-Whitney *p*-values: 0.452 for Normal vs PIN, 0.014 for Normal vs carcinoma, and 0.051 for PIN vs carcinoma. 1000 cells were counted for each tissue (normal, PIN, and carcinoma) for all 51 primary prostate cancer specimens.

Table 3. Quantification of immunohistochemistry staining on prostate tissues.

Prostate Tissue		p16Ink4A +	p16Ink4A -	*p*- value	p14ARF +	p14ARF-	*p*- value
Normal							
	Bmi1+	25.6 ± 5.3%	74.4 ± 8.2%	0.049	55.5 ± 6.7%	44.5 ± 8.3%	0.897
	Bmi1-	52.4 ± 7.4%	47.6 ± 3.5%		51.2 ± 5.6%	48.8 ± 5.2%	
PIN							
	Bmi1+	24.6 ± 8.5%	75.4 ± 6.5%	0.012	35.8 ± 5.1%	64.2 ± 4.2%	0.034
	Bmi1-	65.5 ± 5.9%	34.5 ± 7.8%		59.8 ± 3.4%	40.2 ± 4.5%	
Carcinoma							
	Bmi1+	26.2 ± 4.5%	73.8 ± 6.9%	0.925	30.1 ± 4.0%	69.9 ± 8.0%	0.051
	Bmi1-	25.8 ± 8.0%	74.2 ± 7.7%		44.6 ± 3.2%	55.4 ± 4.5%	

Note: Two-tailed *t*-tests were used to compare the mean percentages of cells stained in the individual tissues. Data presented are mean percentage of cells stained ± SE.

Table 4. Bmi1 promotes DU145 cells to form xenograft tumors in NOD/SCID mice

Cell Type	No. of Tumours per injection	Mean Volume (±SE)[a]
DU145 pBABE	8/8	204 ± 45
DU145 Bmi1	8/8	517 ± 81*

a: mean tumor volume (mm^3) at 4 weeks post-injection

b: significantly greater volume according to a two-tailed independent *t*-test ($p<0.05$)

Figure 1

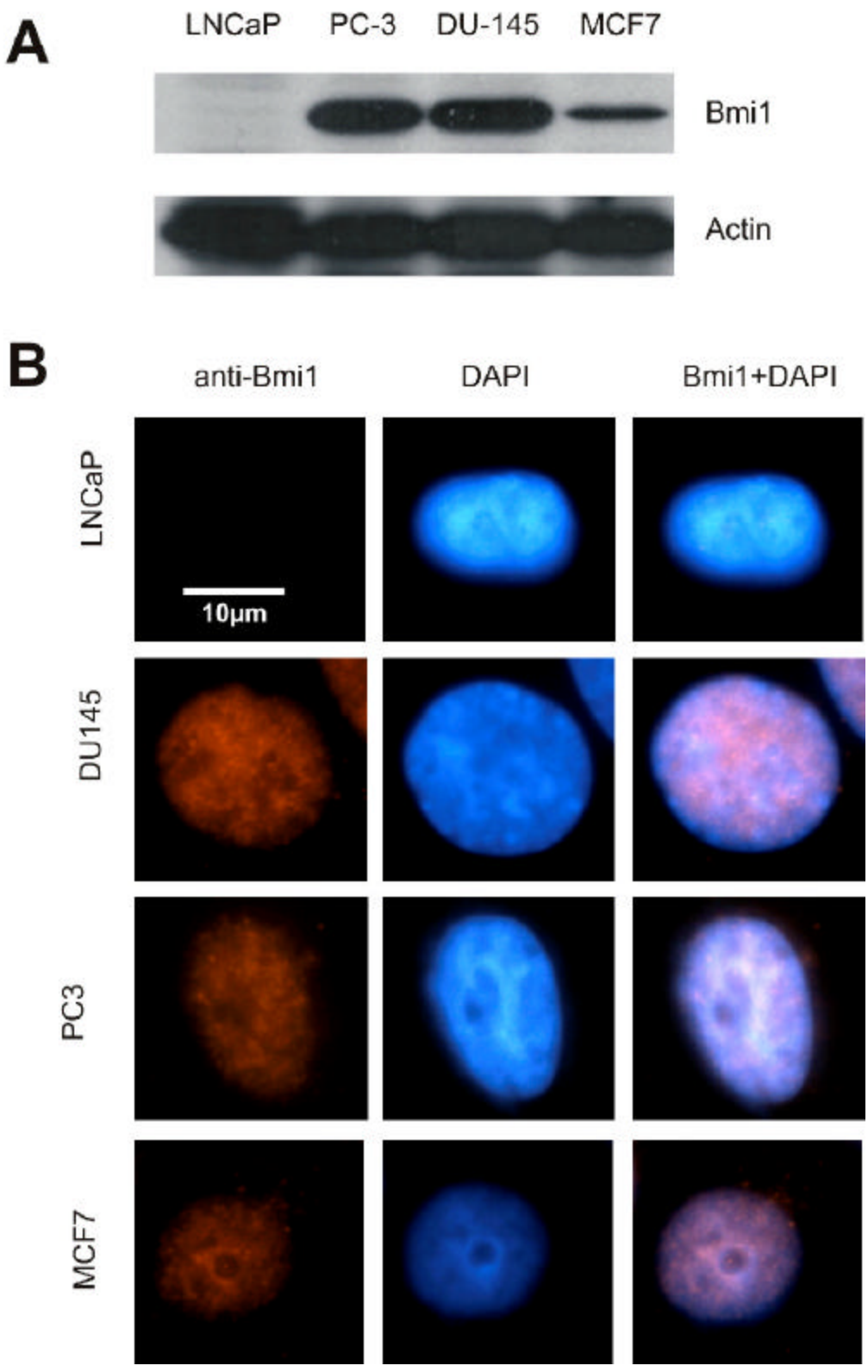

Figure 2

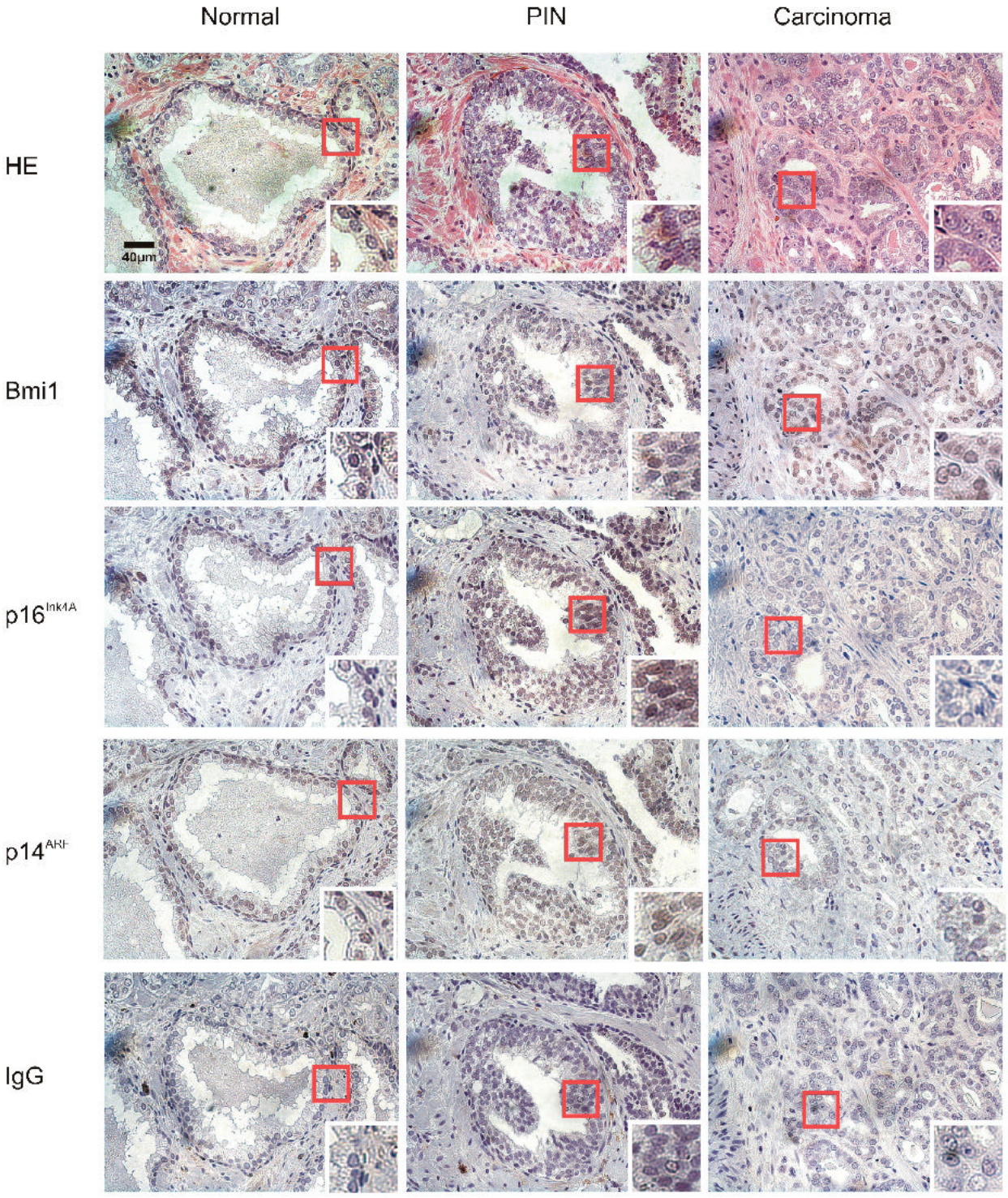

Figure 3